

The LHCb experiment

A. C. dos Reis
on behalf of the LHCb Collaboration



LISHEP 2013

17/3/2013

The LHCb Physics Programme

The purpose of the LHCb experiment is to perform precision tests of the Standard Model and to search for New Physics.

Historically, new particles have first been observed through their virtual effects (e.g., CP violation in the kaon system). This approach probes higher mass scales than direct searches.

LHCb explores the high precision frontier, complementary to ATLAS and CMS, which explore the high energy limit.

LHCb: an experiment designed for the study of rare decays and CP violation in hadrons containing quarks c and b .

Two important questions:

- Does the CP-violating phase of the CKM matrix account for all known CP-violating processes?
- Is the CKM matrix with its four parameters capable to describe all FCNC processes?

Answers to these questions involve some key measurements:

- 1) CP-violating angle γ from in tree-level decays ($B \rightarrow DK$, free from NP);
- 2) mixing-induced CP-violating phase in $B_s^0 \rightarrow J/\psi \phi$;
- 3) analysis of $B_s^0 \rightarrow \phi \gamma$ and other radiative decays;
- 4) analysis of the rare decays $B_{(s)}^0 \rightarrow \mu^+ \mu^-$ and $B^0 \rightarrow K^{*0} \mu^+ \mu^-$;
- 5) BR's and CP asymmetries of $H_b \rightarrow h^+ h'^-$, ($H_b = B_{(s)}^0, \Lambda_b$, $h = K, \pi, \rho$).

100 publications, almost all with 2011 data only:

- $B^0 - \bar{B}^0$ mixing and CP violation;
- $D^0 - \bar{D}^0$ mixing and CP violation in neutral and charged D s;
- radiative and other rare B decays and D decays, LFV searches;
- masses and branching fractions of b - and c -hadrons;
- Dalitz plot analysis;
- B_c physics;
- charmonium and bottomonium production;
- open charm and beauty production and spectroscopy;
- b - and c -baryon spectroscopy, production and polarization;
- new hadrons (X(3872), Z(4330), etc...);
- forward jets;
- W and Z production, electroweak physics...

A comprehensive programme in heavy flavor physics!

Don't miss the very interesting LHCb talks:

Production in the forward direction

M. Rangel, today at 16:40

Mixing and CP violation in charm system

M. Combes, Wednesday at 10:50

Rare decays

F. Polci, Wednesday at 11:20

CP violation in $B_{(s)}^0$ to final states including charmonia

B. Paula, Wednesday at 14:00

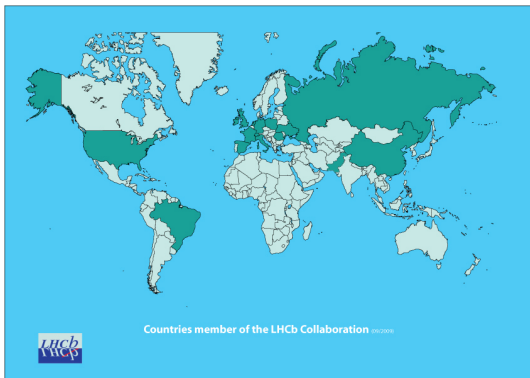
CP violation in charmless hadronic B decays

F. Rodrigues, Wednesday at 14:30

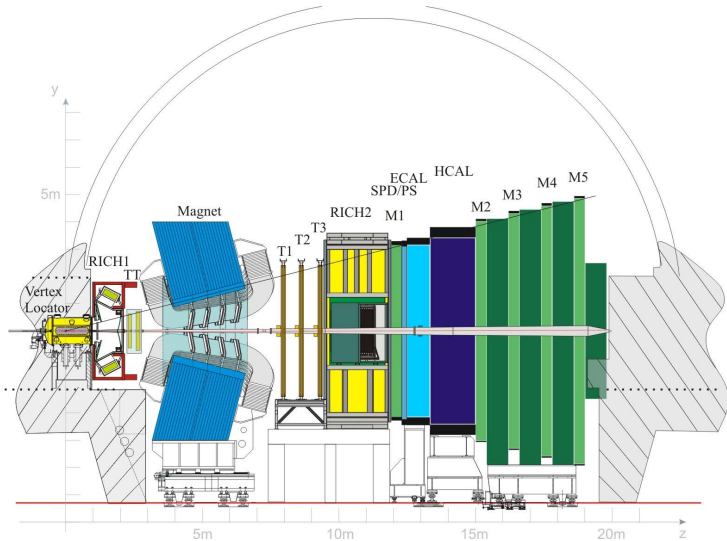
The LHCb upgrade

A. Massafferri, Thursday at 11:30

The LHCb Experiment



16 countries
60 institutes
819 members



LHCb acceptance: $2 < \eta < 5$

At 7 TeV : $\sigma_{pp}^{\text{inel}} \sim 60 \text{ mb}$

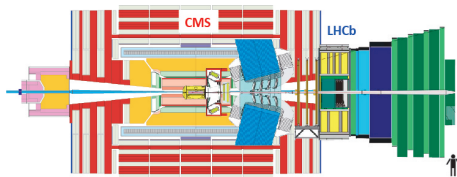
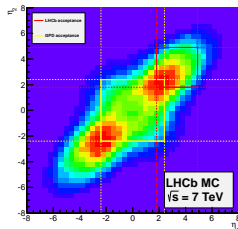
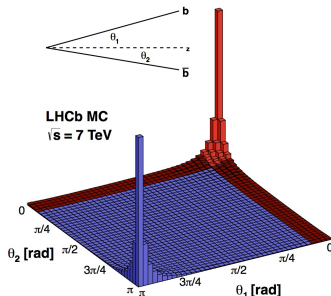
$\sigma(pp \rightarrow c\bar{c}X) \sim 6 \text{ mb}$

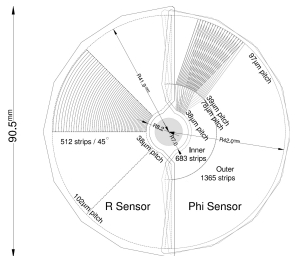
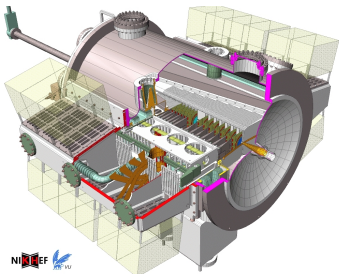
$\sigma(pp \rightarrow b\bar{b}X) \sim 0.3 \text{ mb}$

$\sim 30\%$ within LHCb acceptance:

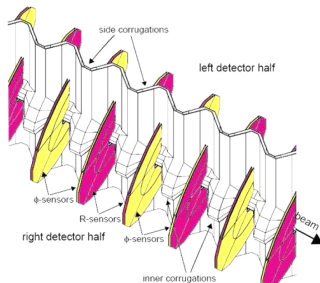
$\sigma(pp \rightarrow b\bar{b}X) = (89.6 \pm 6.4 \pm 15.5) \mu\text{b}$

PLB 684 (2010) 209

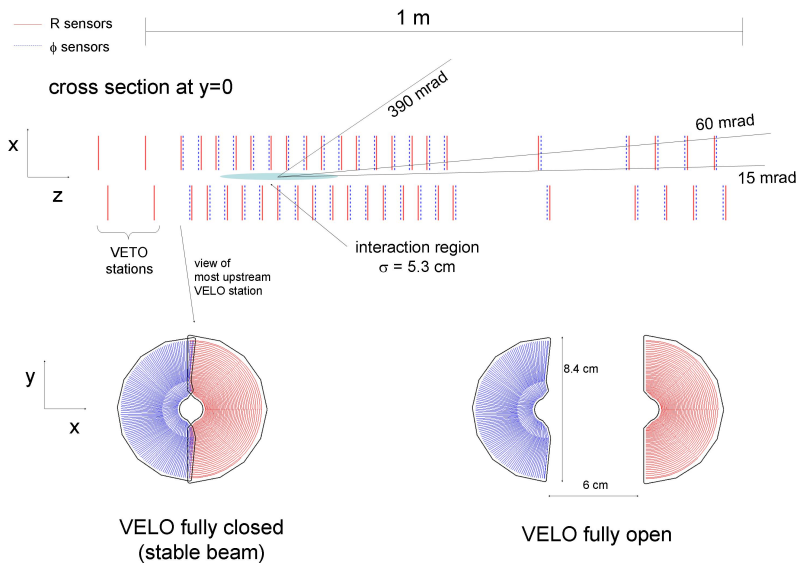




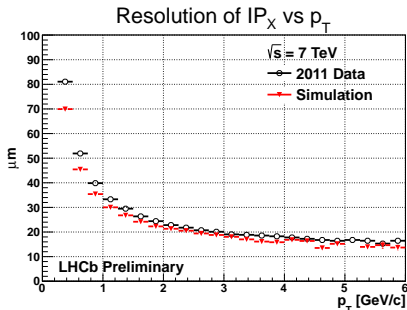
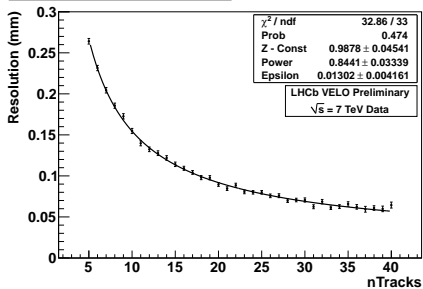
- 2 retractable halves at 8 (60) mm from beam when closed (open);
- 21 stations with double-sided modules (R and ϕ sensors);
- cylindrical geometry allows fast reconstruction for triggering.



Vertex Location - VELO



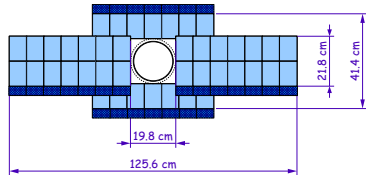
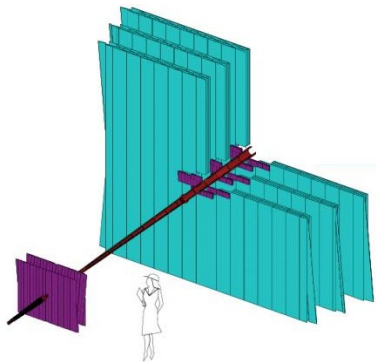
Z resolution - offline, many PVs



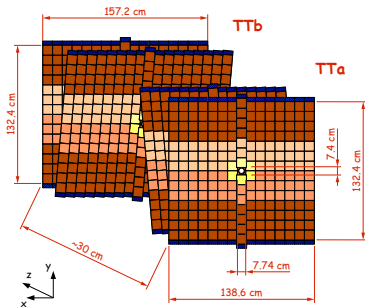
Tracking efficiency above 98%.

z resolution of $\sim 80 \mu\text{m}$ for primary vertices with 25 tracks.

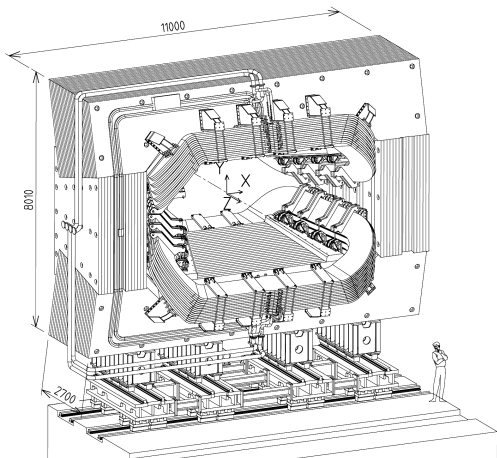
IP resolution of $\sim 22 \mu\text{m}$ for tracks with $p_T > 2 \text{ GeV}/c$.



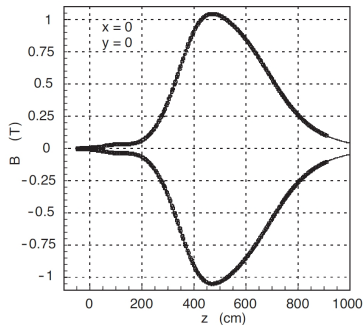
- 1 upstream station (TT) equipped with silicon micro-strips;
- 3 downstream stations (T1-3) with silicon micro-strips in the inner region (IT) and straw tubes (OT) in the outer part.



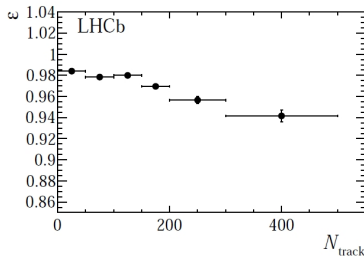
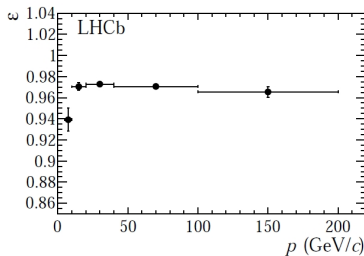
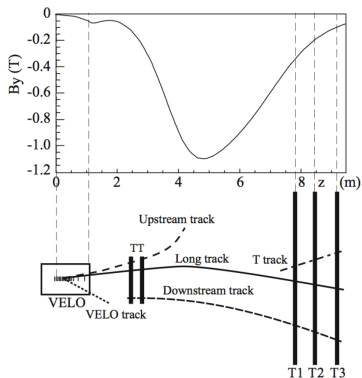
The dipole magnet



- acceptance: ± 250 mrad vertically, ± 300 mrad horizontally (the bending plane);
- $\int B dl = 4 \text{ Tm}$
for tracks of 10 m length;
- $\delta B/B \sim 4 \times 10^{-4}$



Tracking performance

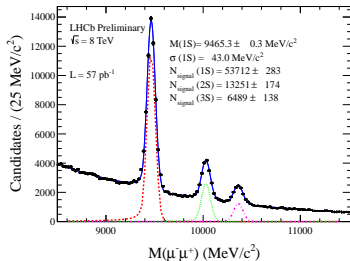
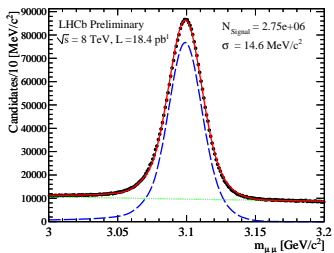


LHCb-PUB-2011-025

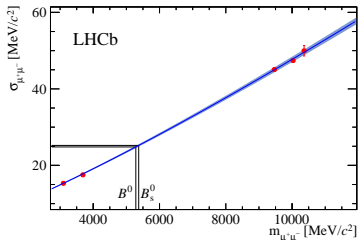
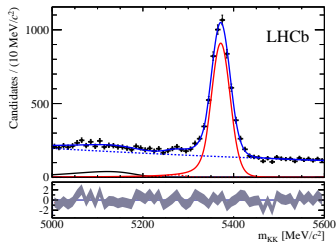
Tracking efficiency measured from data ($J/\psi \rightarrow \mu^+ \mu^-$).

Efficiency $> 96\%$ for long tracks (depends on p , p_T , multiplicity).

Momentum and mass resolution



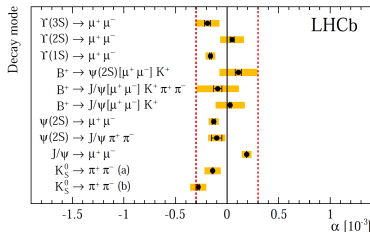
- $\delta p/p$: 0.4 - 0.6% (5-100 GeV/c);
- $\sigma_{\mu\mu} = 15 \text{ MeV}/c^2$ for J/ψ ;



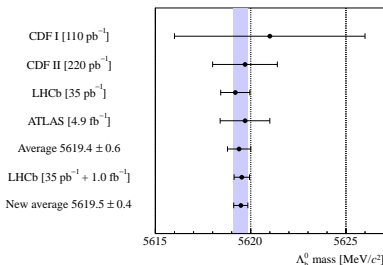
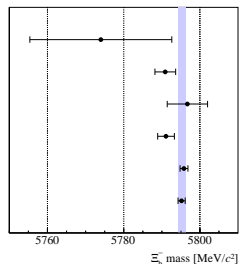
- $\sigma \sim 22 \text{ MeV}/c^2$ for $B \rightarrow hh$;
- $\sigma_{\mu\mu} = 43 \text{ GeV}/c^2$ for $\Upsilon(1S)$;

LHCb-CONF-2012-025, PRL 110, 021801 (2013)

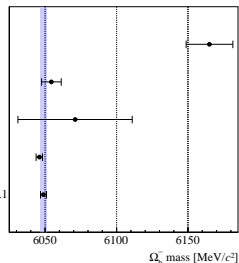
Uncertainties in the magnetic field and tracker alignment imply a small bias in the momentum scale (α). The momentum scale is calibrated using $B^+ \rightarrow J/\psi K^+$.



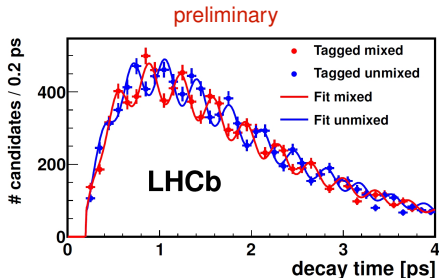
D0 [1.3 fb $^{-1}$]
 CDF [4.2 fb $^{-1}$] $\Xi_b^- \rightarrow J/\psi \Xi^-$
 CDF [4.2 fb $^{-1}$] $\Xi_b^- \rightarrow \Xi_b^0 \pi^-$
 PDG [2012] 5791.1 ± 2.2
 LHCb [1.0 fb $^{-1}$]
 New average 5795.2 ± 0.9



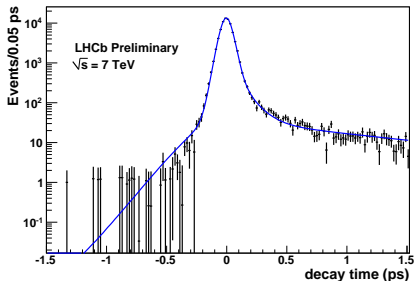
D0 [1.3 fb $^{-1}$]
 CDF [4.2 fb $^{-1}$]
 PDG [2012] 6071 ± 40
 LHCb [1.0 fb $^{-1}$]
 CDF+LHCb average 6048.9 ± 2.1



The excellent vertex resolution translates into an excellent proper time resolution, necessary to measure the fast oscillation frequency of the $B_s^0 - \bar{B}_s^0$ mixing.



LHCb-PAPER-2013-006 (in preparation)

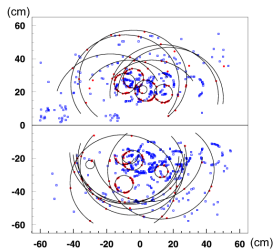
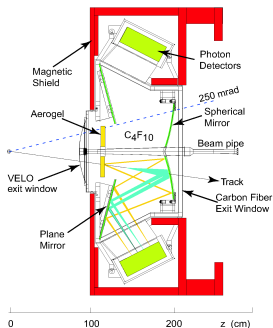


LHCb-CONF-2012-002

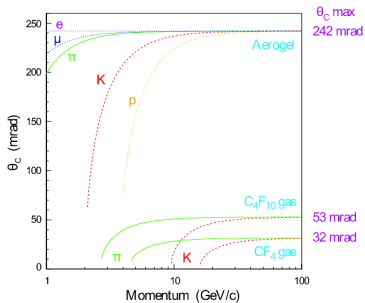
The decay time resolution is measured from data fitting the decay time distribution of $B_s^0 \rightarrow J/\psi\phi$. The time dependent signal PDF is convolved with a Gaussian distribution.

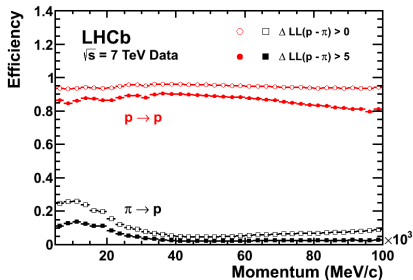
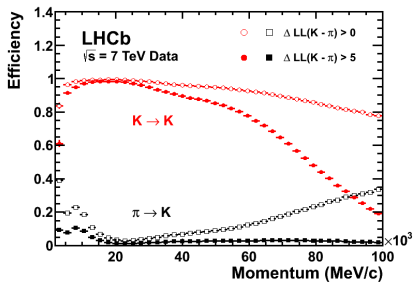
Decay time resolution of 45 fs for $B_s^0 \rightarrow J/\psi\phi$ and $B_s^0 \rightarrow D_s\pi$.

Charged particle identification



- Two Ring Imaging **C**herenkov detectors (RICH1,2);
- RICH1 (upstream) operating with 2 different radiators, aerogel and C₄F₁₀ - low momentum particles;
- RICH2 (downstream): CF₄ - high momentum particles.





- efficiency and misID rates measured directly from data:

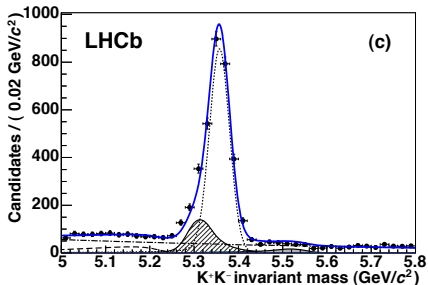
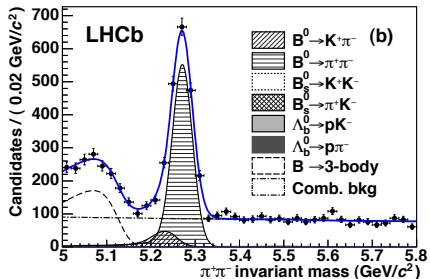
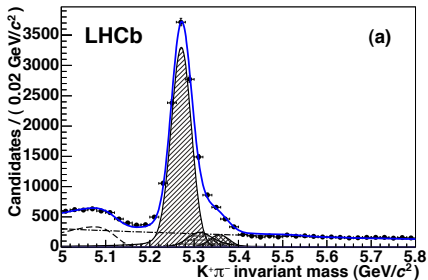
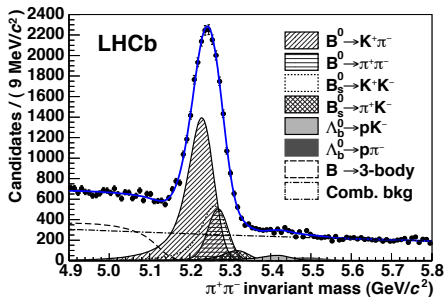
$$K_S^0 \rightarrow \pi^+ \pi^-,$$

$$D^{*+} \rightarrow D^0 (K^- \pi^+) \pi^+,$$

$$\Lambda^0 \rightarrow p \pi^-$$

- $K - \pi$ and $p - \pi$ separation up to 100 GeV/c;
- Kaon ID efficiency $\sim 95\%$ for $\sim 5\%$ pion contamination.

Charged particle identification: $B^0 \rightarrow hh$



JHEP 10 (2012) 037

Scintillator Pad Detector / Pre Shower

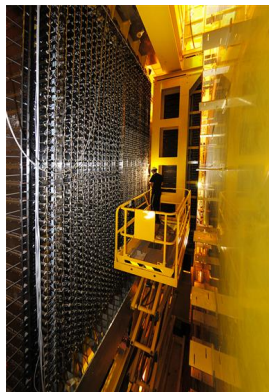
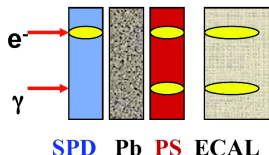
- $e - \gamma$ and e -hadron separation;
- single layer scintillator tiles with a Pb sheet ($2.5 X_0$);
- $\epsilon(e^\pm) \sim 90\%$ for 5% e -hadron misid.

Electromagnetic CALorimeter

- $e - \gamma$ energy measurement;
- Pb plates + scintillator tiles ($25 X_0$);
- $\sigma(E)/E = 10\%/\sqrt{E}$ (GeV) + 1%

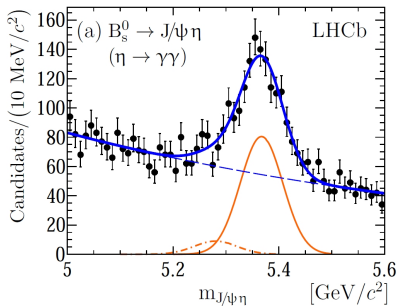
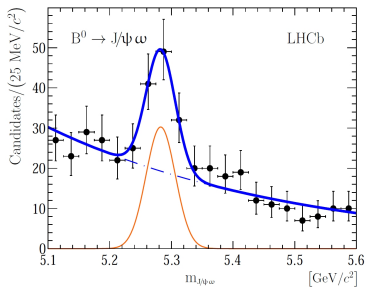
Hadronic CALorimeter

- energy measurement for level 0 trigger;
- Fe plates + scintillator tiles;
- $\sigma(E)/E = 69\%/\sqrt{E}$ (GeV) + 9%

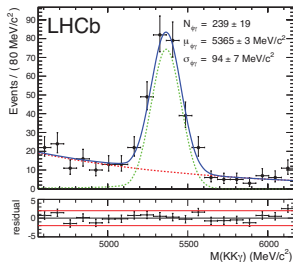
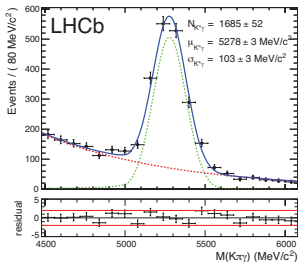


The ECAL detector

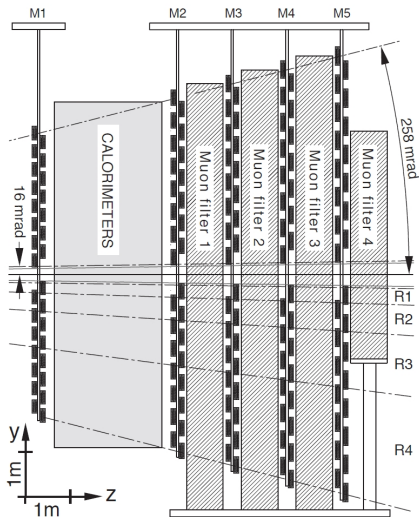
Calorimeters performance



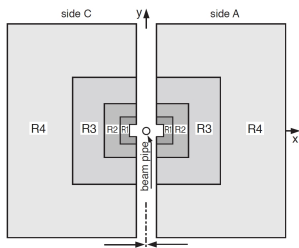
arXiv:1210.2631



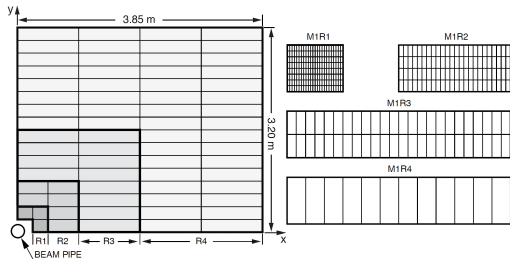
PRD 85 (2012) 112013



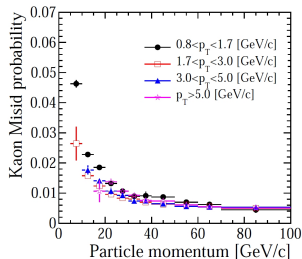
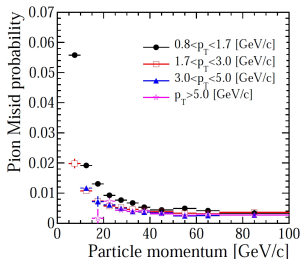
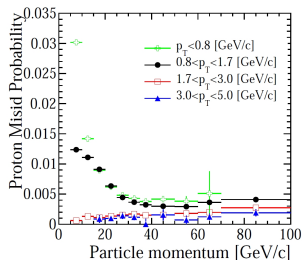
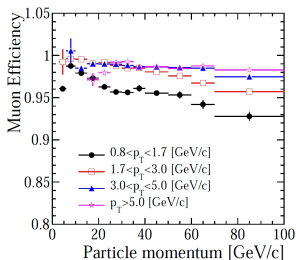
- 1 station before the calorimeters equipped with GEM (inner part) and MWPC detectors;
- all others equipped with MWPCs (double-sided), interleaved by iron walls;
- as in the Calo system, projective geometry, covering the maximum LHCb acceptance;
- variable granularity according to track density;



Granularity depending on particle density:

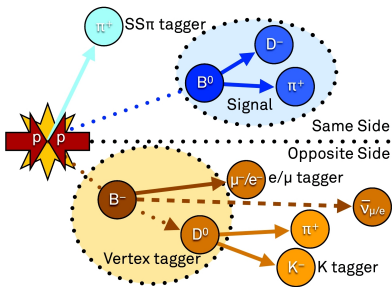


- 435 m² of instrumented area;
- 1380 chambers of 20 different types;
- physical channels combined into 55296 logical pads;
- chambers efficiency above 99%;



muon ID efficiency: $\sim 97\%$ for 1-3% $\pi \rightarrow \mu$ misID probability.

Flavour tagging at production: a necessary condition for measurements of oscillations and time-dependent asymmetries of $B_{(s)}^0$ mesons.



Combination of several algorithms:

Same Side tagging: correlations between "fragmentation tracks" of signal b quark. Pions for $B_{U,d}$ and kaons for B_S .

Opposite Side tagging: information from the decay products of the other (tagging) B in the event. Independent of the signal B .

The performance of the tagging algorithm is determined by the effective tagging efficiency, or tagging power, ϵ_{eff} ,

$$\epsilon_{\text{eff}} = \epsilon_{\text{tag}}(1 - 2\omega)^2 = \epsilon_{\text{tag}}\mathcal{D}_{\text{tag}}^2, \quad \epsilon_{\text{tag}} = \frac{R + W}{R + W + U}, \quad \omega = \frac{W}{R + W},$$

$R, W, U = \text{right, wrong, untagged}$

The effective OS tagging efficiency is measured from the flavor specific decay $B^+ \rightarrow J/\psi K^+$, and cross-checked with $B^0 \rightarrow D^{*-}\mu^+\nu$ and $B^0 \rightarrow J/\psi K^{*0}$,

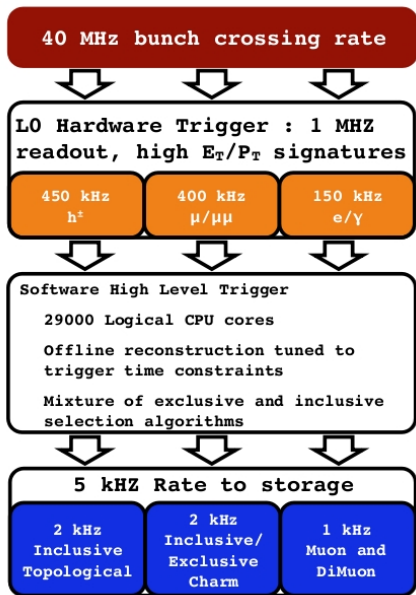
$$\epsilon_{\text{eff}}^{\text{OS}} = (2.35 \pm 0.6)\% \quad \text{EPJ C72 (2012) 2022}$$

The effective SSK tagging efficiency is measured from $B_s^0 \rightarrow D_s^- \pi^+$,

$$\epsilon_{\text{eff}}^{\text{SSK}} = (1.5 \pm 0.4)\% \quad \text{LHCB-CONF-2012-033}$$

The combination of SSK and OS taggers for $B_s^0 \rightarrow D_s^- \pi^+$ yield

$$\epsilon_{\text{eff}} = (3.8 \pm 0.7)\%$$



L0: hardware trigger based on calorimeters and muon systems.

Selects events with high E_T HCAL or ECAL clusters; high p_T muons.

$\sim 4\mu\text{s}$ latency, up to 1 MHz output.

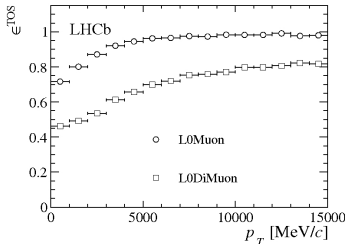
HLT: two-stage software application running on 15K processors. Consists of independent trigger "lines".

HLT1: partial event reconstruction, inclusive selection algorithms.

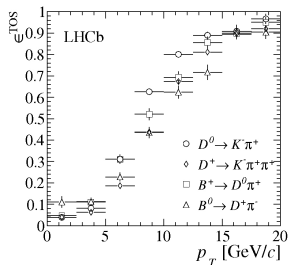
HLT2: full event reconstruction, inclusive and exclusive selections.

decision in ~ 30 ms, rate of 5 kHz

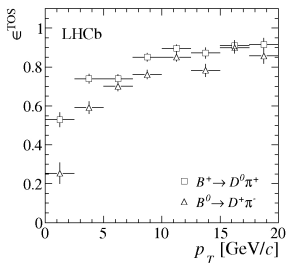
L0: $B^+ \rightarrow J/\psi K^+$



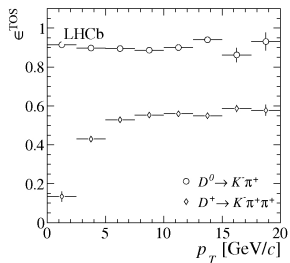
L0: hadronic channels



HLT2: Topo lines

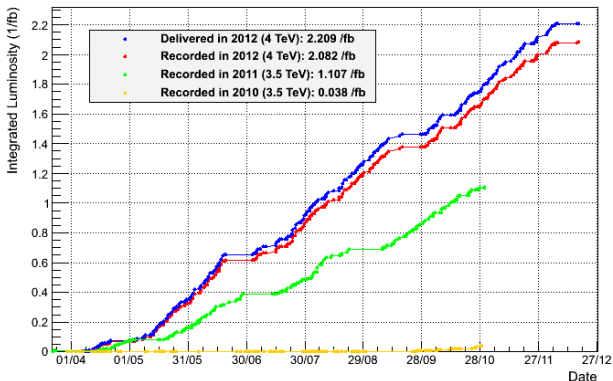


HLT2: charm



arXiv:1211.3055

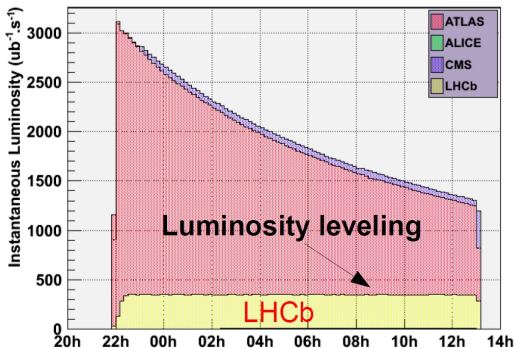
LHCb Integrated Luminosity pp collisions 2010-2012



Luminosity: $2-4 \times 10^{32} \text{ cm}^2 \text{ s}^{-1}$.

Visible interactions/bunch crossing : $\langle \mu \rangle \sim 1.4-1.6$

Magnet polarity reversed periodically.



Beam displacement kept instantaneous luminosity constant.

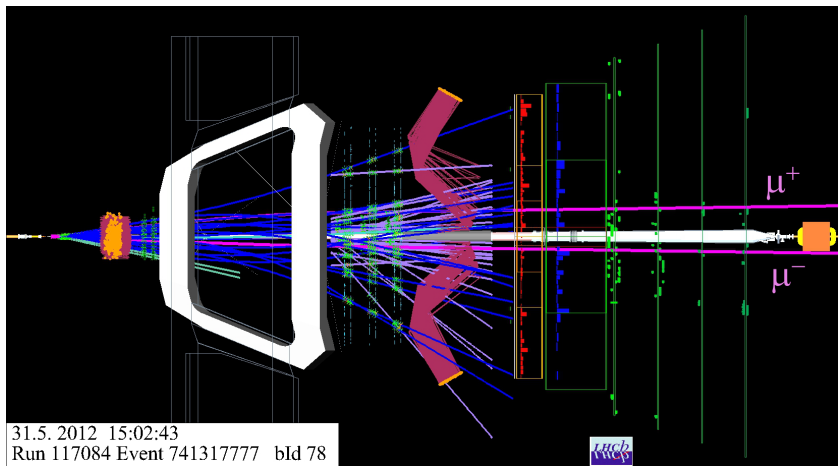
- $\sim 99\%$ of working channels for all subdetectors;
- data taking efficiency over 90%;
- over 99% of data taken is good for analysis;

2011 (7 TeV): 1.0 fb^{-1}

2012 (8 TeV): 2 fb^{-1}

Selected results

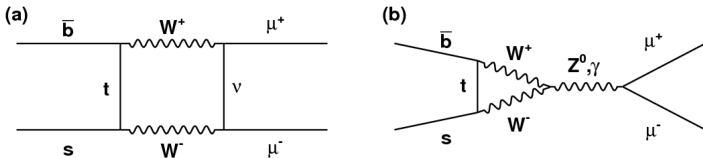
$$B_{(s)}^0 \rightarrow \mu^+ \mu^-$$



1.0 fb⁻¹ (7 TeV) + 1.1 fb⁻¹ (8 TeV).

$B_{(s)}^0 \rightarrow \mu^+ \mu^-$ in the SM

In the SM FCNC processes can only occur via diagrams with quantum loops:



SM predictions of $\mathcal{B}(B_{(s)}^0 \rightarrow \mu^- \mu^+)$ are computed with good accuracy:

$$A(B \rightarrow \mu\mu) = \langle \mu\mu | \mathcal{H}_{\text{eff}} | B \rangle, \quad \mathcal{H}_{\text{eff}} = -\frac{4G_F}{\sqrt{2}} V_{tb} V_{tq}^* \frac{e^2}{16\pi} \sum_i (C_i O_i) + \text{h.c.},$$

$$\mathcal{B}(B^0 \rightarrow \mu^- \mu^+) = (1.07 \pm 0.10) \times 10^{-10},$$

$$\mathcal{B}(B_s^0 \rightarrow \mu^- \mu^+) = (3.23 \pm 0.27) \times 10^{-9}.$$

Buras et al., arXiv:1208.0934

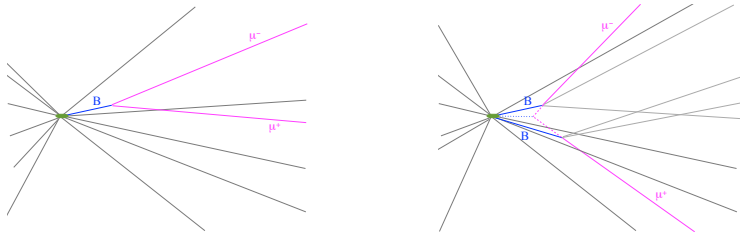
The finite difference in the B_s^0 and \bar{B}_s^0 lifetimes introduce a small correction,

$$\mathcal{B}(B_s^0 \rightarrow \mu^- \mu^+) = (3.54 \pm 0.30) \times 10^{-9}.$$

De Bruyn et al., PRL 109, 041801 (2012)

New particles contributing to the loops could significantly increase branching ratios:

$$\mathcal{H}_{\text{eff}} = -\frac{4G_F}{\sqrt{2}} V_{tb} V_{tq}^* \frac{e^2}{16\pi} \sum_i (C_i O_i + C'_i O'_i) + \text{h.c.},$$



Initial loose selection: two high quality muon candidates (track χ^2 , p_T , IP and μ ID) forming a well detached vertex (χ^2 , IP, FD) (rejects most of the background);

A two-stage multivariate selection (BDT) is applied to the $B_{(s)}^0 \rightarrow \mu^+ \mu^-$ candidates. BDT is trained using $B_{(s)}^0 \rightarrow \mu^+ \mu^-$ MC for signal and $b\bar{b} \rightarrow \mu^+ \mu^- X$ for background.

The probability of an event to have a given value of BDT output is extracted from data using $B_{(s)}^0 \rightarrow h_1^+ h_2^-$, $h_i = K, \pi$, for signal, and sideband $B_{(s)}^0 \rightarrow \mu^+ \mu^-$ for background.

The first step removes 80% of remaining background. The second step and the dimuon invariant mass classify the remaining candidates in a 2-dimensional space.

The number of observed events is compared to the number of expected signal and background events in bins of the BDT output and $m_{\mu\mu}$.

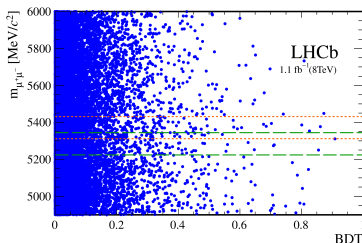
$B_{(s)}^0 \rightarrow \mu^+ \mu^-$ - selection and analysis strategy

Background estimation:

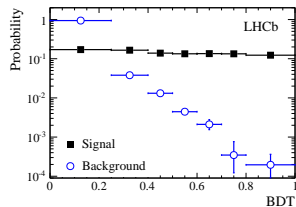
combinatorial $b\bar{b} \rightarrow \mu^+ \mu^- X$;

various exclusive backgrounds: $B_{(s)}^0 \rightarrow h_1^+ h_2^-$, $B^+ \rightarrow \pi^- \mu^+ \nu$, $B_s^0 \rightarrow K^- \mu^+ \nu$,
 $B^{0(+)} \rightarrow \pi^{0(+)} \mu^+ \mu^-$, $\Lambda_b^0 \rightarrow \pi^- \mu^+ \nu$, $B_c^+ \rightarrow J/\psi \mu^+ \nu$.

This analysis: $\varepsilon(\mu \rightarrow \mu) \sim 98\%$, $\varepsilon(\pi \rightarrow \mu) \sim 0.6\%$, $\varepsilon(K \rightarrow \mu) \sim \varepsilon(\rho \rightarrow \mu) \sim 0.3\%$.



For signal and background, the BDT output is independent of the invariant mass.



Signal BDT distribution is nearly uniform.

Background shape peaks at zero.

$B_{(s)}^0$ peak position from $B_{(s)}^0 \rightarrow h_1^+ h_2^-$.

Mass resolution: interpolation of dimuon resonances ($\psi(nS)$, $\Upsilon(nS)$) and $B_{(s)}^0 \rightarrow h_1^+ h_2^-$.

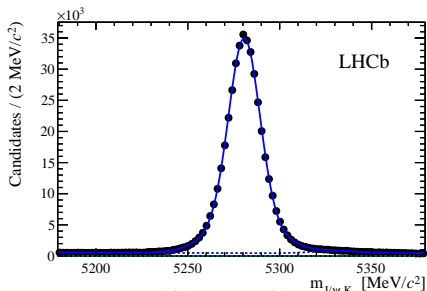
$B_{(s)}^0 \rightarrow \mu^+ \mu^-$ - normalization

The number of observed events is translated into a branching ratio using

$$B = B_{\text{norm}} \times \frac{\epsilon_{\text{norm}}^{\text{rec}} \epsilon_{\text{norm}}^{\text{sel|rec}} \epsilon_{\text{norm}}^{\text{trg|sel}}}{\epsilon_{\text{sig}}^{\text{rec}} \epsilon_{\text{sig}}^{\text{sel|rec}} \epsilon_{\text{sig}}^{\text{trg|sel}}} \times \frac{f_{\text{norm}}}{f_{d(s)}} \times \frac{N_{B_{(s)}^0 \rightarrow \mu^+ \mu^-}}{N_{\text{norm}}},$$

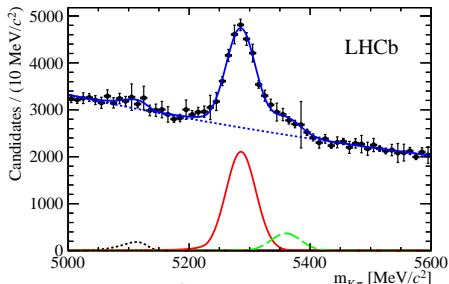
$\epsilon_{\text{norm}/\text{sig}}^{\text{rec}}, \epsilon_{\text{norm}/\text{sig}}^{\text{sel|rec}} \rightarrow \text{MC}$

$\epsilon_{\text{norm}/\text{sig}}^{\text{trg|sel}} \rightarrow \text{data}$



$B^+ \rightarrow J/\psi K^+$

Similar trigger, different topology



$B^0 \rightarrow K^+ \pi^-$

different trigger, same topology.

f_d/f_s : ratio of $B_S^0 \rightarrow D_S \mu X$ to $B \rightarrow D^+ \mu X$;
ratio of $B_S^0 \rightarrow D_S^+ \pi^-$ to $B^0 \rightarrow D^- K^+, D^- \pi^+$

Combined result: $f_d/f_s = 0.256 \pm 0.020$ (PRD 85 (2012) 032008, LHCb-PAPER-2012-037)

$B^0 \rightarrow \mu^+ \mu^-$ - results

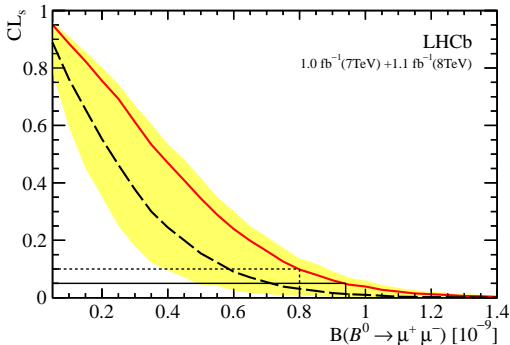
The compatibility between the observed and expected distribution of events is computed using the CL_s method.

95% CL upper limit: $CL_s = 0.05$

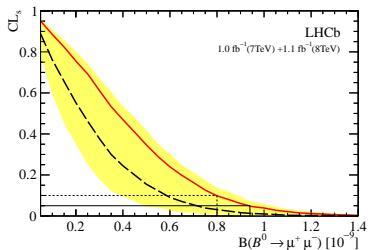
$CL_b \rightarrow$ background-only hypothesis;

$CL_{s+b} \rightarrow$ signal+background hypothesis;

$CL_s = CL_{s+b}/CL_b$.



$B(B^0 \rightarrow \mu^+ \mu^-) < 9.4 \times 10^{-10}$ at 95% CL

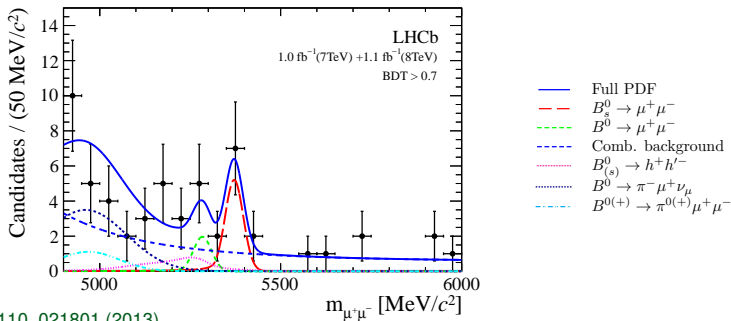


$$\text{SM: } (3.54 \pm 0.3) \times 10^{-9}$$

$$B(B_s^0 \rightarrow \mu^+ \mu^-) = (3.2_{-1.2}^{+1.4} {}_{-0.3}^{+0.5}) \times 10^{-9}$$

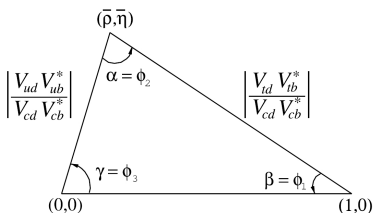
p-value for bkg-only: 5.3×10^{-4}

a 3.5σ excess,
first evidence!



PRL 110, 021801 (2013)

Measurements of γ using tree-mediated decays



$$\gamma = \arg \left[-V_{ud} V_{ub}^* / (V_{cd} V_{cb}^*) \right]$$

γ is the least well constrained angle:

$$(66 \pm 12)^\circ \text{ (CKMFitter)}$$

$$(72 \pm 9)^\circ \text{ (UTFitter)}$$

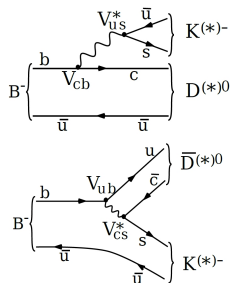
Determination from tree-level decays:
negligible theoretical uncertainty,
 $\mathcal{O}(10^{-6})$, making it a "standard candle".

Several established methods to measure γ in $B \rightarrow DK$ decays.

$B \rightarrow DK = B^+ \rightarrow DK^+, B^0 \rightarrow D^{(*)\mp} \pi^\pm, B_s^0 \rightarrow D_s^\mp K^\pm, B^0 \rightarrow DK^{*0}$ and
 $B_s^0 \rightarrow D\phi$, where D refers to an admixture of D^0 and \bar{D}^0 .

All based on the interference between $b \rightarrow u$
and $b \rightarrow c$ tree amplitudes when $D^0 \rightarrow f \leftarrow \bar{D}^0$.

Best sensitivity obtained combining different methods.



The amplitudes of the $B^- \rightarrow D^0 K^-$ and $B^- \rightarrow \bar{D}^0 K^-$:

$$A(B^- \rightarrow D^0 K^-) = A_c e^{i\delta_c}, \quad A(D^0 \rightarrow f) = A_f e^{i\delta_f},$$

$$A(B^- \rightarrow \bar{D}^0 K^-) = A_u e^{i(\delta_u - \gamma)}, \quad A(D^0 \rightarrow \bar{f}) = A_{\bar{f}} e^{i\delta_{\bar{f}}},$$

$$A(B^- \rightarrow [f]_D K^-) = A_c A_f e^{i(\delta_c + \delta_f)} + A_u A_{\bar{f}} e^{i(\delta_u + \delta_{\bar{f}} - \gamma)}, \quad B^- \rightarrow B^+, \gamma \rightarrow -\gamma$$

The total decay rate is:

$$\Gamma(B^- \rightarrow DK^-) = |A(B^- \rightarrow [f]_D K^-)|^2 \propto A_c^2 \left(A_f^2 + r_B^2 A_{\bar{f}}^2 + 2r_B A_f A_{\bar{f}} \text{Re}(e^{i(\delta_B + \delta_D - \gamma)}) \right),$$

$$r_B = |A(b \rightarrow u)/A(b \rightarrow c)|, \quad \delta_B = \delta_u - \delta_c \quad \text{and} \quad \delta_D = \delta_{\bar{f}} - \delta_f.$$

So far LHCb has analysed different combinations of B/D decays (1.0 fb^{-1} , 7 TeV):

- $B^\pm \rightarrow DK^\pm, D^0 \rightarrow K^- K^+, \pi^- \pi^+, \pi^- K^+$ (GLW/ADS); (PLB 712 (2012) 203)
- $B^\pm \rightarrow DK^\pm, D^0 \rightarrow K^+ \pi^- \pi^+ \pi^-$ (ADS); (LHCb-CONF-2012-030)
- $B^\pm \rightarrow DK^\pm, D^0 \rightarrow K_S \pi^- \pi^+, K_S K^- K^+$ (GGSZ) (PLB 718 (2012) 43);
- $B_s^0 \rightarrow D_s^\mp K^\pm$; (LHCb-CONF-2012-029)
- $B^0 \rightarrow DK^{*0}, D \rightarrow K^+ K^-$. (LHCb-CONF-2012-024)

Observables are ratios of partial widths and CP asymmetries:

$$R_{\text{CP,ADS}} = \frac{\Gamma(B^- \rightarrow DK^-) + \Gamma(B^+ \rightarrow DK^+)}{\Gamma(B^- \rightarrow D^0 K^-) + \Gamma(B^+ \rightarrow \bar{D}^0 K^+)}, \quad A_{\text{CP,ADS}} = \frac{\Gamma(B^- \rightarrow DK^-) - \Gamma(B^+ \rightarrow DK^+)}{\Gamma(B^- \rightarrow D^0 K^-) + \Gamma(B^+ \rightarrow \bar{D}^0 K^+)}$$

$$\text{GLW} \Rightarrow R_{\text{CP}} = 1 + r_B^2 \pm 2r_B \cos \delta_B \cos \gamma,$$

$$A_{\text{CP}} = \pm 2r_B \sin \delta_B \sin \gamma / R_{\text{CP}}.$$

$$\text{ADS} \Rightarrow R_{\text{ADS}} = r_B^2 + r_D^2 + 2r_B r_D \cos \gamma \cos(\delta_B + \delta_D),$$

$$A_{\text{ADS}} = 2r_B r_D \sin \gamma \sin(\delta_B + \delta_D) / R_{\text{ADS}}.$$

$B \rightarrow D\pi$ has limited sensitivity to γ , but it is a convenient control channel used for the ratios

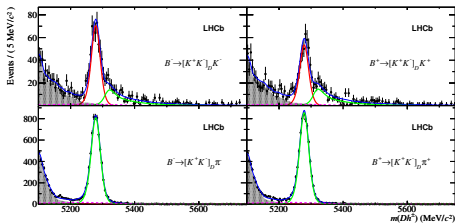
$$R_{K/\pi}^f = \frac{\Gamma(B^- \rightarrow [f]_D K^-) + \Gamma(B^+ \rightarrow [f]_D K^+)}{\Gamma(B^- \rightarrow [f]_D \pi^-) + \Gamma(B^+ \rightarrow [f]_D \pi^+)},$$

from which we compute a weighted average

$$R_{\text{CP}} = \frac{\langle R_{K/\pi}^{KK}, R_{K/\pi}^{\pi\pi} \rangle}{R_{K/\pi}^{K\pi}}.$$

For ADS is more convenient to define the two statistically ratios

$$R_{\pm} \equiv \frac{\Gamma(B^{\pm} \rightarrow [K^{\mp} \pi^{\pm}]_D h^{\pm})}{\Gamma(B^{\pm} \rightarrow [K^{\pm} \pi^{\mp}]_D h^{\pm})} = r_B^2 + r_D^2 + 2r_B r_D \cos(\delta_B + \delta_D \pm \gamma), \quad (h = K, \pi)$$

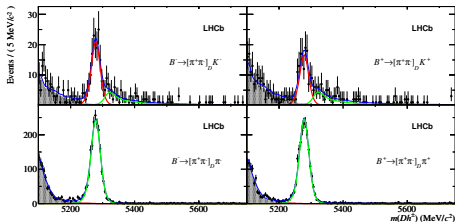


A common multivariate selection (BDT) used for 16 combinations of $B^\pm \rightarrow Dh_1^\pm$, $D \rightarrow h_2^\pm h_3^\mp$

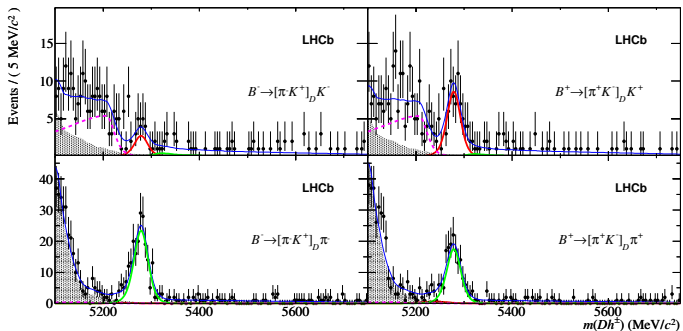
Similar CP asymmetry in KK and $\pi\pi$.

$$A_{CP} = \langle A_K^{KK}, A_K^{\pi\pi} \rangle = 0.145 \pm 0.032 \pm 0.010$$

$$R_{CP} = \frac{\langle R_{K/\pi}^{KK}, R_{K/\pi}^{\pi\pi} \rangle}{R_{K/\pi}^{K/\pi}} = 1.007 \pm 0.038 \pm 0.012$$



PLB 712 (2012), 203



PLB 712 (2012), 203

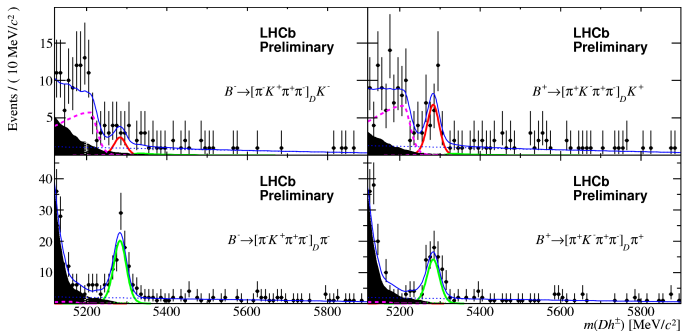
First observation of $B^\pm \rightarrow [\pi^\pm K^\mp]_D K^\pm$.

Direct CPV in $B^\pm \rightarrow DK^\pm$ decays observed with a significance of 5.8σ .

$$A_{\text{ADS}(K)} = (R_K^- - R_K^+) / (R_K^- + R_K^+) = -0.52 \pm 0.15 \pm 0.02.$$

$$A_{\text{ADS}(\pi)} = (R_\pi^- - R_\pi^+) / (R_\pi^- + R_\pi^+) = 0.143 \pm 0.062 \pm 0.011.$$

$r_D = A_f/A_{\bar{f}} = |A(D^0 \rightarrow \pi^- K^+) / A(D^0 \rightarrow K^- \pi^+)|$ and δ_D taken from CLEO-c (arXiv:0903.4853).



LHCb-CONF-2012-030

First observation of $B^\pm \rightarrow [\pi^\pm K^\mp \pi^+ \pi^-]_D \pi^\pm$ and $B^\pm \rightarrow [\pi^\pm K^\mp \pi^+ \pi^-]_D K^\pm$.

Same formalism as for 2-body case, but less sensitivity due to the coherence factor.

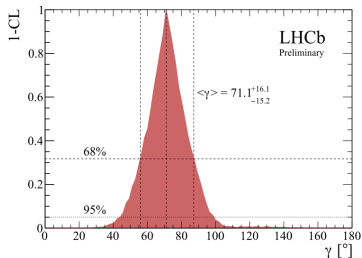
$$A_{\text{ADS}(K)}^{K3\pi} = (R_K^{K3\pi,-} - R_K^{K3\pi,+}) / (R_K^{K3\pi,-} + R_K^{K3\pi,+}) = -0.42 \pm 0.22.$$

$$A_{\text{ADS}(\pi)}^{K3\pi} = (R_\pi^{K3\pi,-} - R_\pi^{K3\pi,+}) / (R_\pi^{K3\pi,-} + R_\pi^{K3\pi,+}) = 0.13 \pm 0.10.$$

(Statistical and systematic errors combined.)

Combining $B \rightarrow DK$ results (1.0 fb^{-1} at $\sqrt{s} = 7 \text{ TeV}$)

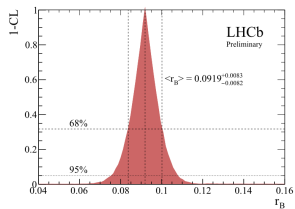
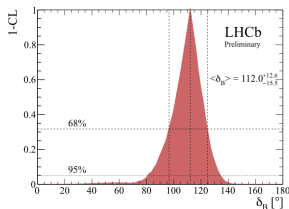
A frequentist approach was used for the combination with additional input from CLEO-c for the $D \rightarrow K\pi$ and $D \rightarrow K\pi\pi\pi$ decay parameters (PRD80,031105 (2009)).



$$\gamma = (71.1^{+16.6}_{-15.7})^\circ,$$

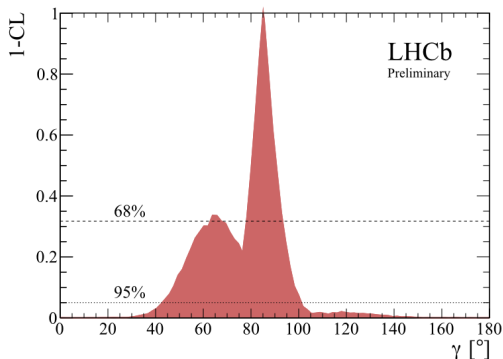
$$r_B = 0.092 \pm 0.008,$$

$$\delta_B = 112.0^{+12.6}_{-15.5}(\circ).$$



LHCb-CONF-2012-032

When $B \rightarrow DK$ and $B \rightarrow D\pi$ measurements are combined a new solution appears at 1σ . The best-fit value of γ is shifted to 85.1° . The 2σ interval remains stable.



LHCb-CONF-2012-032

γ	63.7°	85.1°
68% CL	$[61.8, 67.8]^\circ$	$[77.9, 92.4]^\circ$
95% CL	$\leftarrow [43.8, 101.5]^\circ \rightarrow$	
$r_{B(K)}$	0.0948	
68% CL	$[0.0860, 0.1032]$	
95% CL	$[0.078, 0.111]$	
$\delta_{B(K)}$	119.0°	
68% CL	$[107.0, 129.1]^\circ$	
95% CL	$[79.7, 137.9]^\circ$	
$r_{B(\pi)}$	0.0239	
68% CL	$[0.0153, 0.0310]$	
95% CL	$[0.0, 0.037]$	
$\delta_{B(\pi)}$	373.7°	321.4°
68% CL	$[365.7, 387.0]^\circ$	$[311.2, 328.4]^\circ$
95% CL	$\leftarrow [160.5, 333.6]^\circ \rightarrow$	

The whole 2012 data set is to be analysed.
 Many other decay modes are to be added.

Thanks to the superb performance of the LHC, to the levelling technique and to the excellent performance of the LHCb detector we have on disk over 3 fb^{-1} of high quality data.

So far most public results have only the 2011 data and are already the most precise individual measurements, or even more accurate than the previous world averages.

Analysis of the core physics channels is well advanced.
So far the SM remains unchallenged.

Great prospects for CP violation and flavor physics measurements in the near future, in both b and c sectors.
Lots of fresh results in the pipeline.

LHCb: an experiment with plenty of opportunities!

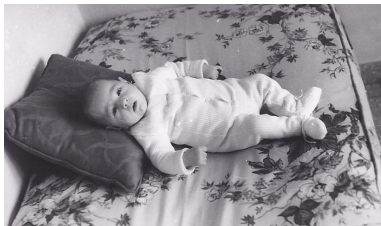
Javier Edgardo Magnin



In memoriam

1963-2012

Javier was born in 1963 in Necochea, Argentina.

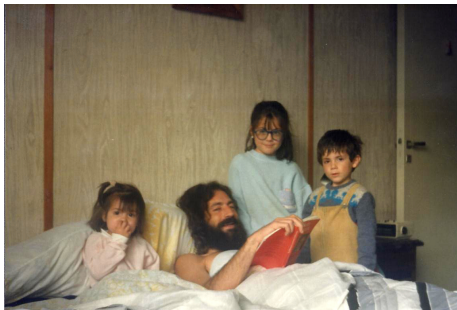




He got his degree in Physics at
Universidad de San Luis;



In 1994 he got his PhD degree at
Instituto Balseiro, Bariloche, under the
supervision of Luis Masperi.



Still in Argentina he had
three beautiful sons:

Ana, Maria Ines and Andres;



In 1995 he came to CBPF as a
PosDoc. At that time he was
interested in the production
mechanisms of polarized hyperons.

In the same year he joined
his first HEP experiment:

Fermilab E791,
our first common project;



In 1999, after his PosDoc at CBPF, he took a position in Universidad de los Andes, Bogota, Colombia, as Assistant Professor.

He maintained a strong collaboration with other Latin American groups, especially with Colombia and Mexico, in theoretical physics.

Having multiple interests and skills, he worked on various topics as hadron structure, quark-gluon plasma, charm production, computing, electronics...



In 2003 Javier joined LHCb. He managed to reconcile an intense teaching activity with theoretical research and with his experimental activities. He was the first one to propose a charm program at LHCb.

He played a decisive role in the creation of the CBPF GRID, and was the main responsible for the creation of the Resource Operator Center for Latin American, ROC_LA.



From his second marriage Javier had two new "daughters".



Farewell, "Pibe"!